Single Base Station Tracking Approaches with Hybrid TOA/AOD/AOA Measurements in Different Propagation Environments

Shixun Wu, Miao Zhang, Kanapathippillai Cumanan, Kai Xu, and Zhangli Lan

***Abstract*—In this paper, mobile terminal (MT) tracking based on time of arrival (TOA), angle of departure (AOD), and angle of arrival (AOA) measurements with one base station is investigated. The main challenge is the unknown propagation environment, such as line-of-sight (LOS), non-line-of-sight (NLOS) modeled as one-bounce scattering or mixed LOS/NLOS propagations, which may result in heterogeneous measurements. For LOS scenario, a linear Kalman filter (LKF) algorithm is adopted through analyzing and deriving the estimated error of MT. For NLOS scenario, as the position of scatterer is unknown, a nonlinear range equation is formulated to measure the actual AOD/AOA measurements and the position of scatterer, and three different algorithms: The extended Kalman filter (EKF), unscented Kalman filter (UKF) and an approximated LKF are developed. For mixed LOS/NLOS scenario, the modified interacting multiple model LKF (M-IMM-LKF) and the identified LKF algorithms (I-LKF) are utilized to address the issue of the frequent transition between LOS and NLOS propagations. In comparison with EKF and UKF algorithms, the simulation results and running time comparisons show the superiority and effectiveness of the LKF algorithm in LOS and NLOS scenarios. Both M-IMM-LKF and I-LKF algorithms are capable to significantly reduce the localization errors, and better than three existing algorithms.**

***Index Terms*—Extended Kalman filter (EKF), interacting multiple model (IMM), linear Kalman filter (LKF), non-line-of-sight (NLOS), tracking, unscented Kalman filter (UKF).**

I. Introduction

PRECISE mobile terminal (MT) tracking is one of the key technologies that has numerous practical applications, such as emergency rescues, intelligent transportation systems, location-based services, as well as several commercial or military applications. The most widely utilized MT tracking approaches are based on the received signal strength (RSS), time of arrival (TOA), time difference of arrival (TDOA), and angle of arrival (AOA) measurements [1]–[5].

The main challenge for precise MT tracking is the non-line-of-sight (NLOS) propagation, where the line-of-sight (LOS) propagation between transmitter and receivers are blocked by different obstacles. A significant research work has been focused on this problem, which can be mainly divided into two groups, single measurement and hybrid measurements. For single measurement, MT tracking is achieved with a single type of measurement, i.e., TOA, TDOA, AOA or RSS. A linear Kalman-based interacting multiple model (IMM) algorithm is proposed in [6] to smooth the NLOS range measurement, which can accurately estimate the range distance between base station (BS) and MT. However, the NLOS range errors are assumed to be Gaussian random variables with known mean and variance. The work in [7] employs the estimated range errors for NLOS detection, where two biased extended Kalman filter (EKF) algorithms with NLOS mitigation are proposed. Due to the unknown condition of LOS or NLOS propagation, particle filter (PF) method is exploited to estimate the unknown condition, and then EKF is applied in [8]. The work in [9] utilizes the modified EKF to jointly estimate the state of MT and propagation condition, and a Bayesian data fusion algorithm is exploited to further reduce the tracking errors. For NLOS errors with the assumption of definite but unknown distributions, a Rao-blackwellized PF and parameter learning method is proposed in [10]. In [11], a robust EKF algorithm with robust regression for NLOS scenario is proposed, then by collaborating with another EKF algorithm, an IMM-based algorithm is formulated for mixed LOS/NLOS scenario. The work in [12] presents a method to distinguish NLOS measurements from LOS measurementss with standard deviation of range measurements and K-means clustering, where LOS measurement is reconstructed by polynomial fitting, and a novel EKF algorithm is developed. Utilizing the measured parameters of multipath, a multipath-assisted tracking algorithm for long-term evolution (LTE) systems is proposed in [13]. The cooperative localization method for tracking problems is investigated in [14], where a semi-definite programming (SDP) based cooperative tracking algorithm is proposed to mitigate the NLOS error. A novel NLOS identification algorithm based on distributed filtering and data association is studied in [15] to mitigate the effect of NLOS propagation. In [16], the multi-sensory single cluster filter is exploited to recursively estimate the state of MT and map feature, and a PF is presented. By utilizing biased feature of min-max algorithm, a hybrid constrained Kalman filter based on linear Kalman filter (LKF)

Manuscript received June 3, 2024; revised August 24, 2024; approved for publication by Xia, Xiang-Gen Division 1 Editor, September 26, 2024.

This work was supported in part by the Natural Science Foundation of Chongqing under grant number CSTB2024NSCQ-MSX0275, in part by the National Nature Science Foundation of China under Grant No. 62101080, in part by the Chongqing Municipal Education Commission under Grant No. KJQN202100738 and in part by the Chongqing Science and Technology Bureau under Grant No. CSTB2022BSXM-JCX0113. The work of K. Cumanan was supported by the UK Engineering and Physical Sciences Research Council (EPSRC) under grant number EP/X01309X/1.

S. Wu, M. Zhang, K. Xu, and Z. Lan are with the School of Information Science and Engineering, Chongqing Jiaotong University, Chongqing, 400074, China, email: wushixun333@163.com, msczz@foxmail.com, xkxjxwx@hotmail.com, 385551137@qq.com.

K. Cumanan is with the School of Physics, Engineering and Technology, University of York, York, UK, email: kanapathippillai.cumanan@york.ac.uk.

S. Wu is the corresponding author.

Digital Object Identifier: 10.23919/JCN.2024.000053

1229-2470/24/$10.00 © 2024 KICS

and unscented Kalman filter (UKF) is investigated in [17]. Integrating Gaussian mixture model (GMM), IMM, and EKF, a Gaussian IMM-EKF algorithm is proposed to address the problem of the frequent transitions of range measurement between LOS and NLOS in [18]. Hypothesis testing is used for NLOS identification, an enhanced closest neighbor data association approach combined with PF is proposed in [19].

For hybrid measurements, the MT tracking can be achieved through multiple systems or multiple types of measurements, such as global navigation satellite system (GNSS)/cellular network, TOA/AOA, TDOA/AOA, TOA/RSS, etc. Three different EKF filter algorithms only with LOS propagation are evaluated by hybrid positioning which is based on signals from satellites and BSs [20]. In [21], NLOS identification and Kalman filter-based mitigation methods are utilized to reduce the NLOS error. An AOA selection process is used to deal with the effects of inaccurate NLOS AOA measurement, then a hybrid TDOA/AOA tracking algorithm based on EKF is presented to mitigate the effect of NLOS error. Combining EKF with IMM algorithm for accurately smoothing range estimate between BSs and MT, an extended Kalman-based IMM tracking algorithm with hybrid TOA/RSS measurement is proposed to mitigate the NLOS effects in [22]. By introducing a slack variable into motion state and considering the relationship between this variable and the position estimate, a hybrid unified Kalman tracking algorithm is developed with hybrid TOA/TDOA measurements in [23]. A hybrid scheme in an urban scenario with GNSS and cellular network is presented in [24], where the EKF algorithm is used to integrate the TDOA measurements from the cellular network and the pseudorange measurements from GNSS.

Despite the approaches from the above mentioned works have the capability to effectively reduce the impact of NLOS errors, the hearability problem [6] may be a critical issue due to the assumption that there are three or more BSs involved in the tracking process. When a MT is near the serving BS, it must reduce its power to avoid causing interference to other users. However, too weak transmitted power may not be received by three or more nearby BSs to estimate the position of MT. In addition, involving multiple BSs simultaneously in the tracking process will result in additional information exchange overhead and latency [25], [26]. Fortunately, with emerging millimeter-wave technique for the fifth generation (5G) and beyond, it is possible to track the position of MT with one BS by exploiting TOA, AOA, and angle of departure (AOD) measurements [27]–[29], when both BS and MT are equipped with multiple antennas or array of antenna. The hybrid TOA/AOD/AOA localization method utilizing a single BS can be broadly classified into two categories: static positioning and dynamic tracking. The main challenge is the unknown propagation environment, i.e., LOS, one-bounce (OB) or multi-bounce (MB) scattering. For static positioning, under the premise of OB scattering, a nonlinear constrained optimization localization approach is present to reduce the feasible search area of solution by leveraging AOD and AOA measurements [30]. By exploiting the geometric relation between AOD and AOA, a theoretic threshold is derived to decide whether the propagation path is LOS or NLOS. Subsequently, a data fusion localization algorithm, incorporating residual weighting, is employed to process both LOS and OB scattering measurements [31]. The estimated errors of OB scattering paths are derived, a linear cooperative localization algorithm is proposed by one-order Taylor expansion in [32]. When the MB scattering is present, without the synchronization between MT and BS, the work in [33] proposes a double identification algorithm to identify and discard the MB path. Meanwhile, an ensemble learning-based model is proposed to classify the LOS, OB, or MB paths using 5G channel parameters [34]. Moreover, an iterative weighted least square is proposed to mitigate the effects of MB paths with different weights [35]. It is noteworthy that the aforementioned works operate under the assumption of a multipath environment, where only LOS and OB paths are deemed conducive to enhancing positioning accuracy.

For dynamic tracking, an EKF tracking algorithm with the position of scatters is proposed in [36], premised on stationary scatterers and OB environment. With the assumption of LOS and OB NLOS paths, a radio-environmental mapping assisted PF is proposed to accurately estimate the position of MT as well as nearby scatterers [27]. However, the positions of MT and scatterer are integrated into the state space, resulting in a high dimensional unknown parameter space. A nonlinear least squares method is employed to estimate the position of MT and the orientation relative to the BS, subsequently leveraging a LKF to perform MT tracking [37]. The time bias is introduced, an ordinary differential equation (ODE) solver integrated with a long short-term memory (LSTM) network is proposed to achieve continuous and precise tracking [38]. Nevertheless, these approaches primarily focus on OB paths. In a multipath environment, when a LOS path is available, its measured parameters offer superior suitability and reliability for tracking compared to OB paths, even though OB paths can contribute to improved tracking performance. In the absence of a LOS path, OB paths are utilized for tracking. Due to the uncertainty surrounding scatterers, only one path is typically considered. To the best of our knowledge, none of the existing works has considered developing a hybrid TOA/AOD/AOA tracking approach with single BS and one path.

In this paper, we distinguish our approach from prior works in [27], [36] by excluding the position of scatterers in the state space model for the OB NLOS environment. Furthermore, we analyze the scenarios involving LOS or OB paths without considering MB paths, which are more relevant to practical applications than the works in [37], [38] that only OB path is present. This choice is justified by two reasons. On the one hand, MB paths with significant attenuation and weaker signal strengths are infrequent in millimeter-wave frequencies, as noted in [27], [39]. On the other hand, LOS or OB paths can be effectively distinguished within a multipath environment, as demonstrated in [33], [34]. Hence, we investigate three distinct propagation environments, i.e., LOS, OB or hybrid LOS/OB propagation environment. The primary challenges for hybrid TOA/AOD/AOA tracking lie in the unknown position of scatterers in NLOS scenarios and the frequent transitions between LOS and NLOS propagation. To tackle these challenges, an approximated LKF is utilized to deal with the

unknown position of scatterer, while the modified interacting multiple model LKF (M-IMM-LKF) and the identified LKF algorithms (I-LKF) are exploited to address the issue of the frequent transition between LOS and NLOS propagation. Our contributions can be summarized as follows:

1) Firstly, for LOS environment, hybrid TOA/AOD/AOA measurements is divided into two combinations, each combination can estimate the position of MT with the geometry relation, and a new LKF algorithm is proposed to track the position of MT by deriving the estimated error of MT.
2) Secondly, for NLOS environment, the NLOS propagation is modeled as OB scattering. Due to the unknown position of scatterer, the nonlinear relationship between position of scatterer and the actual AOD/AOA measurements is constructed. Plugging this relationship and the position of BS into NLOS TOA measurement equation, a new nonlinear measurement equation is defined. Similarly, the EKF and UKF algorithms can be directly realized to track the position of MT with this new measurement equation. However, due to the high computational complexity of UKF and low tracking accuracy of EKF, an approximated LKF algorithm is proposed by utilizing the geometric feature among the actual TOA/AOD/AOA measurements.
3) Thirdly, for mixed LOS/NLOS environment, the key issue is the frequent transition between LOS and NLOS, which leads to the large tracking error. To address this issue, M-IMM-LKF and I-LKF algorithms based on the developed LOS and NLOS LKF algorithms are proposed.
4) Finally, extensive simulation results are conducted to evaluate the performance of the developed algorithms. The proposed LKF algorithms show the better tracking accuracy and lower running time than EKF algorithm in LOS or NLOS environment. Additionally, the M-IMM-LKF and I-LKF algorithms can reduce the tracking error in mixed LOS and NLOS environment, when the transition between LOS and NLOS occurs.

The rest of this paper is organized as follows. In Section II, state and measurement models are presented. Section III demonstrates the EKF algorithm and derives the LKF algorithm for LOS environment. Section IV develops the EKF, UKF and LKF algorithms for NLOS environment. In Section V, two new algorithms referred to as M-IMM-LKF and I-LKF are presented. Section VI provides simulation results to demonstrate the effectiveness of the proposed algorithms. Finally, conclusions are drawn in Section VII.

II. System Model

A. State Model

In this paper, we consider a moving MT with motion state $X(k) = [x(k), y(k), \dot{x(k)}, \dot{y(k)}]^T$, where $(x(k), y(k))$ denote the horizontal and vertical coordinates of MT at time instant k, $(\dot{x(k)}, \dot{y(k)})$ are the corresponding horizontal and vertical velocities. The MT served by home BS is moving on a 2D-plane and its movement with random acceleration can be modeled as [6]–[12], [20], [21]

$$X(k) = A \cdot X(k-1) + G \cdot W(k-1), \tag{1}$$

where

$$A = \begin{bmatrix} 1 & 0 & \Delta t & 0 \\ 0 & 1 & 0 & \Delta t \\ 0 & 0 & 1 & 0 \\ 0 & 0 & 0 & 1 \end{bmatrix}, G = \begin{bmatrix} \Delta t^2/2 & 0 \\ 0 & \Delta t^2/2 \\ \Delta t & 0 \\ 0 & \Delta t \end{bmatrix},$$

and Δt is the sampling period. The vector-valued processing noise $W(k-1) = [w_x(k-1), w_y(k-1)]^T$ is assumed to be a Gaussian random variable with zero mean and covariance $Q = \sigma_w^2 \cdot I_{2\times 2}$, where $I_{2\times 2}$ is a 2×2 identity matrix.

B. Measurement Model

The signal propagation between the BS and the MT is LOS or OB scattering, as shown in Fig. 1. The MT transmits the signal to the serving BS while trying to localize itself. From the development of multiple-input multiple-output (MIMO) and millimeter wave techniques, we can obtain three parameters, i.e., the measured range, the AOD and the AOA of the propagation path [26], [40]. Therefore, when the signal experiences LOS propagation path, its mathematical expressions are given by

$$\begin{aligned} r(k) &= \sqrt{(x(k)-x_1)^2 + (y(k)-y_1)^2} + n(k) \\ &= r^0(k) + n(k) = c \cdot t(k), \\ \alpha(k) &= \alpha^0(k) + m(k), \\ \beta(k) &= \beta^0(k) + v(k), \end{aligned} \tag{2}$$

$$\alpha^0(k) = \begin{cases} atan(\frac{y_1 - y(k)}{x_1 - x(k)}), & x_1 \geq x(k),\ y_1 \geq y(k), \\ \pi + atan(\frac{y_1 - y(k)}{x_1 - x(k)}), & x_1 < x(k),\ y_1 \geq y(k), \\ \pi + atan(\frac{y_1 - y(k)}{x_1 - x(k)}), & x_1 < x(k),\ y_1 < y(k), \\ 2\pi + atan(\frac{y_1 - y(k)}{x_1 - x(k)}), & x_1 \geq x(k),\ y_1 < y(k), \end{cases}$$

$$\beta^0(k) = \begin{cases} atan(\frac{y(k) - y_1}{x(k) - x_1}), & x(k) \geq x_1,\ y(k) \geq y_1, \\ \pi + atan(\frac{y(k) - y_1}{x(k) - x_1}), & x(k) < x_1,\ y(k) \geq y_1, \\ \pi + atan(\frac{y(k) - y_1}{x(k) - x_1}), & x(k) < x_1,\ y(k) < y_1, \\ 2\pi + atan(\frac{y(k) - y_1}{x(k) - x_1}), & x(k) \geq x_1,\ y(k) < y_1, \end{cases}$$

where (x_1, y_1) is the position of home BS, c is the speed of light, $t(k)$, $\alpha(k)$, and $\beta(k)$ are the measured TOA, AOD, and AOA parameters, respectively. The $r^0(k)$, $\alpha^0(k)$, and $\beta^0(k)$ denote the actual range, the AOD and the AOA, respectively, whereas $atan$ is the function of inverse tangent. The $n(k)$, $m(k)$, and $v(k)$ are white Gaussian random variables with the standard deviation σ_n, σ_α, and σ_β, respectively.

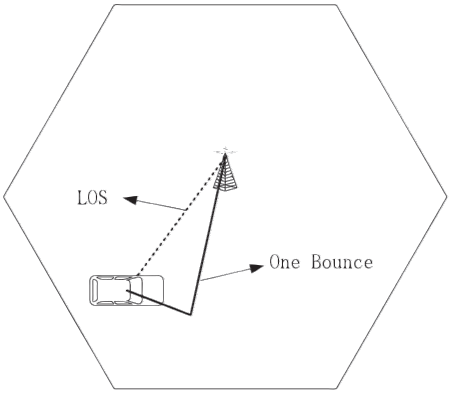

Fig. 1. Measurement model with LOS or OB scattering path.

However, for the signal experiencing OB scattering path [26], [29]–[42], the mathematical expressions can be provided as

$$\begin{aligned} r(k) =& \sqrt{(x(k)-x^{'}(k))^2+(y(k)-y^{'}(k))^2} \\ &+\sqrt{(x_1-x^{'}(k))^2+(y_1-y^{'}(k))^2}+n(k) \\ =& r^0(k)+n(k)=c\cdot t(k), \\ \alpha(k) =& \alpha^0(k)+m(k), \\ \beta(k) =& \beta^0(k)+v(k), \end{aligned} \tag{3}$$

$$\alpha^0(k)=\begin{cases} atan\left(\dfrac{y^{'}(k)-y(k)}{x^{'}(k)-x(k)}\right), & x^{'}(k)\geq x(k),\ y^{'}(k)\geq y(k), \\ \pi+atan\left(\dfrac{y^{'}(k)-y(k)}{x^{'}(k)-x(k)}\right), & x^{'}(k)< x(k),\ y^{'}(k)\geq y(k), \\ \pi+atan\left(\dfrac{y^{'}(k)-y(k)}{x^{'}(k)-x(k)}\right), & x^{'}(k)< x(k),\ y^{'}(k)< y(k), \\ 2\pi+atan\left(\dfrac{y^{'}(k)-y(k)}{x^{'}(k)-x(k)}\right), & x^{'}(k)\geq x(k),\ y^{'}(k)< y(k), \end{cases}$$

$$\beta^0(k)=\begin{cases} atan(\frac{y^{'}(k)-y_1}{x^{'}(k)-x_1}), & x^{'}(k)\geq x_1,\ y^{'}(k)\geq y_1, \\ \pi+atan(\frac{y^{'}(k)-y_1}{x^{'}(k)-x_1}), & x^{'}(k))< x_1,\ y^{'}(k)\geq y_1, \\ \pi+atan(\frac{y^{'}(k)-y_1}{x^{'}(k)-x_1}), & x^{'}(k)< x_1,\ y^{'}(k)< y_1, \\ 2\pi+atan(\frac{y^{'}(k)-y_1}{x^{'}(k)-x_1}), & x^{'}(k)\geq x_1,\ y^{'}(k)< y_1, \end{cases}$$

where $(x^{'}(k), y^{'}(k))$ is the unknown position of the scatterer at time k.

The continuous motion of MT inherently results in dynamic variations within the propagation paths. In addition, in a multipath environment where LOS path is absent, one OB path is typically selected for MT tracking. However, it cannot guarantee that an OB path with similar scattering characteristics will consistently be chosen at any given time. As a result, the random position of scatter is more convincing and adaptable to the different propagation environment.

III. The Proposed Tracking Algorithms with Only LOS Path

In the LOS propagation environment, based on the linear state model defined in (1), we can directly apply the existing algorithms, such as EKF or UKF to track the position of MT with nonlinear measurement parameters that are shown in (2). Since this nonlinear measurement can be adequately approximated utilizing the first-order Taylor series linearization, an EKF is introduced, offering a comparable performance to the UKF while providing a reduced computational burden. Furthermore, leveraging the geometric relationship among TOA/AOD/AOA measurements offers a potential to further enhance the tracking performance.

A. The Tracking Algorithms based on Nonlinear Filtering

The nonlinear measurement parameters defined in (2) can be expressed as a vector form:

$$\mathbf{r}(k)=\mathbf{h}(X(k))+\mathbf{n}(k), \tag{4}$$

where

$$\mathbf{r}(k)=\begin{bmatrix} r(k) \\ \alpha(k) \\ \beta(k) \end{bmatrix}, \mathbf{n}(k)=\begin{bmatrix} n(k) \\ m(k) \\ v(k) \end{bmatrix},$$

$$\mathbf{h}(X(k))=\begin{bmatrix} \sqrt{(x(k)-x_1)^2+(y(k)-y_1)^2} \\ \alpha^0(k) \\ \beta^0(k) \end{bmatrix}.$$

This nonlinear measurement can be linearized around the predicted estimate $\hat{X}(k)$ and it is expressed as

$$\mathbf{h}(X(k))=\mathbf{h}(\hat{X}(k))+H\cdot(X(k)-\hat{X}(k)), \tag{5}$$

where

$$H=[\frac{\partial \mathbf{h}}{\partial x(k)}(\hat{X}(k)), \frac{\partial \mathbf{h}}{\partial y(k)}(\hat{X}(k)), \mathbf{0}_{3\times 1}, \mathbf{0}_{3\times 1}], \tag{6}$$

$$\frac{\partial \mathbf{h}}{\partial x(k)}=\begin{bmatrix} \frac{x(k)-x_1}{\sqrt{(x(k)-x_1)^2+(y(k)-y_1)^2}} \\ -\frac{y(k)-y_1}{(x(k)-x_1)^2+(y(k)-y_1)^2} \\ -\frac{y(k)-y_1}{(x(k)-x_1)^2+(y(k)-y_1)^2} \end{bmatrix},$$

$$\frac{\partial \mathbf{h}}{\partial y(k)}=\begin{bmatrix} \frac{y(k)-y_1}{\sqrt{(x(k)-x_1)^2+(y(k)-y_1)^2}} \\ \frac{x(k)-x_1}{(x(k)-x_1)^2+(y(k)-y_1)^2} \\ \frac{x(k)-x_1}{(x(k)-x_1)^2+(y(k)-y_1)^2} \end{bmatrix}.$$

By substituting (5) into (4), we obtain the approximated measurement equations:

$$\mathbf{r}(k)=\mathbf{h}(\hat{X}(k))+H\cdot(X(k)-\hat{X}(k))+\mathbf{n}(k). \tag{7}$$

The EKF recursive algorithm [36] for LOS propagation environment is summarized in Algorithm 1.

Algorithm 1 LOS-EKF

1: Initialization: $k = 0$, set the state vector $X(0)$ and the covariance $P(0)$;
2: Recursive estimation: For $k = 1, 2, \cdots$
3: Time update: Project the state vector and covariance ahead from (1), $\hat{X}(k) = A \cdot X(k-1)$, $\hat{P}(k) = A \cdot P(k-1) \cdot A^T + G \cdot Q \cdot G^T$;
4: Measurement update: Compute the linear vector H according to (6);
5: Compute the covariance of measurement noise in (5) $R = diag[\sigma_\alpha^2, \sigma_\beta^2, \sigma_n^2]$;
6: Calculate the Kalman gain $K = \hat{P}(k) \cdot H^T \cdot (H \cdot \hat{P}(k) \cdot H^T + R)^{-1}$;
7: Update the state vector and covariance estimate with measurement $\mathbf{r}(k)$ shown in (4) and (7), $X(k) = \hat{X}(k) + K \cdot (\mathbf{r}(k) - \mathbf{h}(\hat{X}(k)))$, $P(k) = \hat{P}(k) - K \cdot H \cdot \hat{P}(k)$;

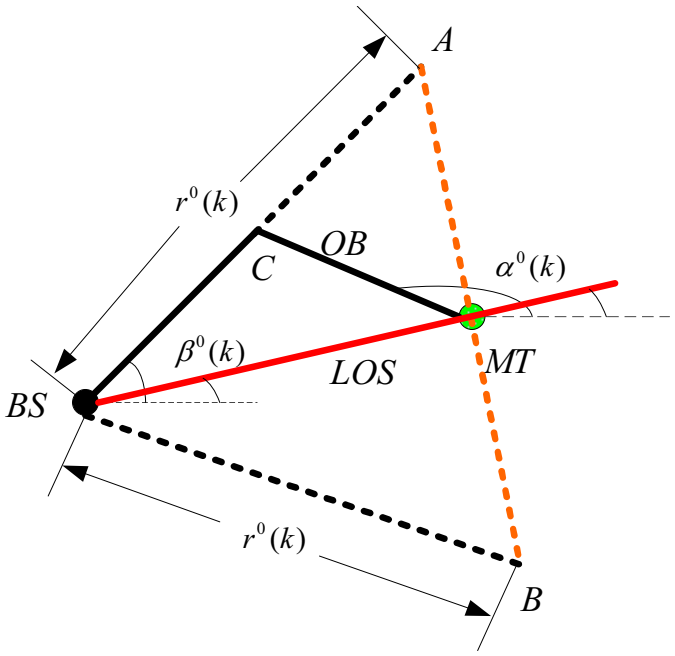

Fig. 2. Possible position of MT with LOS or OB path.

B. The Tracking Algorithms based on Linear Filtering

It is obvious that LOS propagation is the special case of OB scattering. As shown in Fig. 2, when the path is LOS propagation, the scatterer C is on the line of BS and MT, both A and B will converge to the position of MT. Thus, we can utilize the position of A and B to estimate the position of MT. The position of A and B related to the measured model in (2) can be calculated as

$$\begin{pmatrix} x_A \\ y_A \end{pmatrix} = \begin{pmatrix} x_1 \\ y_1 \end{pmatrix} + \begin{pmatrix} r(k) \cdot cos(\beta(k)) \\ r(k) \cdot sin(\beta(k)) \end{pmatrix}, \tag{8}$$

$$\begin{pmatrix} x_B \\ y_B \end{pmatrix} = \begin{pmatrix} x_1 \\ y_1 \end{pmatrix} - \begin{pmatrix} r(k) \cdot cos(\alpha(k)) \\ r(k) \cdot sin(\alpha(k)) \end{pmatrix}. \tag{9}$$

In general, it is assumed that the angle noise $v(k)$ is small. Therefore, we have $cos(v(k)) \approx 1$ and $sin(v(k)) \approx v(k)$. Substituting the angle measurement equations (2) into (8) and dropping the quadratic term of the noise, the following approximation can be obtained

$$\begin{aligned} \begin{pmatrix} x_A \\ y_A \end{pmatrix} &\approx \begin{pmatrix} x_1 \\ y_1 \end{pmatrix} + \begin{pmatrix} r^0(k) \cdot cos(\beta^0(k)) + a_1 \\ r^0(k) \cdot sin(\beta^0(k)) + b_1 \end{pmatrix} \\ &= \begin{pmatrix} x(k) \\ y(k) \end{pmatrix} + \begin{pmatrix} a_1 \\ b_1 \end{pmatrix}, \end{aligned} \tag{10}$$

where $a_1 = -r^0(k) \cdot sin(\beta^0(k)) \cdot v(k) + cos(\beta^0(k)) \cdot n(k)$, $b_1 = r^0(k) \cdot cos(\beta^0(k)) \cdot v(k) + sin(\beta^0(k)) \cdot n(k)$. Similarly, the position of B can be derived as

$$\begin{aligned} \begin{pmatrix} x_B \\ y_B \end{pmatrix} &\approx \begin{pmatrix} x_1 \\ y_1 \end{pmatrix} - \begin{pmatrix} r^0(k) \cdot cos(\alpha^0(k)) + a_2 \\ r^0(k) \cdot sin(\alpha^0(k)) + b_2 \end{pmatrix} \\ &= \begin{pmatrix} x(k) \\ y(k) \end{pmatrix} + \begin{pmatrix} a_2 \\ b_2 \end{pmatrix}, \end{aligned} \tag{11}$$

where $a_2 = r^0(k) \cdot sin(\alpha^0(k)) \cdot m(k) - cos(\alpha^0(k)) \cdot n(k)$, $b_2 = -r^0(k) \cdot cos(\alpha^0(k)) \cdot m(k) - sin(\alpha^0(k)) \cdot n(k)$.

Combining (10) with (11), a new linear measurement equation with matrix form is expressed as

$$Y_1(k) = H_1 \cdot X(k) + S(k), \tag{12}$$

where

$$\begin{aligned} H_1 = \begin{bmatrix} 1 & 0 & 0 & 0 \\ 0 & 1 & 0 & 0 \end{bmatrix}, S(k) = \frac{1}{2} \begin{pmatrix} a_1 + a_2 \\ b_1 + b_2 \end{pmatrix}, \\ Y_1(k) = \frac{1}{2} \left(\begin{pmatrix} x_A \\ y_A \end{pmatrix} + \begin{pmatrix} x_B \\ y_B \end{pmatrix} \right). \end{aligned} \tag{13}$$

Due to the unknown actual range and angles of the vector $S(k)$, we exploit the measured range and angles to replace them. Then, we can express the covariance estimate of $S(k)$ as

$$R = \begin{bmatrix} R_{11} & R_{12} \\ R_{21} & R_{22} \end{bmatrix}, \tag{14}$$

where

$$\begin{aligned} R_{11} = &\frac{1}{4}((cos(\beta(k)) - cos(\alpha(k)))^2 \cdot \sigma_n^2 + (r(k) \cdot sin(\alpha(k)))^2 \\ &\times \sigma_\alpha^2 + (r(k) \cdot sin(\beta(k)))^2 \cdot \sigma_\beta^2), \end{aligned} \tag{15}$$

$$\begin{aligned} R_{22} = &\\ &\frac{1}{4}((sin(\beta(k)) - sin(\alpha(k)))^2 \times \sigma_n^2 + (r(k) \cdot cos(\alpha(k)))^2 \\ &\times \sigma_\alpha^2 + (r(k) \cdot cos(\beta(k)))^2 \cdot \sigma_\beta^2), \end{aligned} \tag{16}$$

$$\begin{aligned} R_{12} = R_{21} = &\\ &\frac{1}{4}((cos(\beta(k)) - cos(\alpha(k))) \cdot (sin(\beta(k)) \\ &- sin(\alpha(k))) \cdot \sigma_n^2 - r(k)^2 \cdot sin(\alpha(k)) \cdot cos(\alpha(k)) \\ &\times \sigma_\alpha^2 - r(k)^2 \cdot sin(\beta(k)) \cdot cos(\beta(k)) \cdot \sigma_\beta^2). \end{aligned} \tag{17}$$

From (8) to (17), the TOA/AOD/AOA measurements are strategically segregated into two distinct combinations:

Algorithm 2 LOS-LKF

1: Initialization: $k = 0$, set the state vector $X(0)$ and the covariance $P(0)$;
2: Recursive estimation: For $k = 1, 2, \cdots$
3: Time update: Project the state vector and covariance ahead from (1), $\hat{X}(k) = A \cdot X(k-1)$, $\hat{P}(k) = A \cdot P(k-1) \cdot A^T + G \cdot Q \cdot G^T$;
4: Measurement update: Compute the new measurement $Y_1(k)$ according to (8), (9), and (13);
5: Compute the covariance estimate of $S(k)$ according to (14), (15), (16), and (17);
6: Calculate the Kalman gain $K = \hat{P}(k) \cdot H_1^T \cdot (H_1 \cdot \hat{P}(k) \cdot H_1^T + R)^{-1}$;
7: Update the state vector and covariance estimate, $X(k) = \hat{X}(k) + K \cdot (Y_1(k) - H_1 \cdot \hat{X}(k))$, $P(k) = \hat{P}(k) - K \cdot H_1 \cdot \hat{P}(k)$;

TOA/AOD and TOA/AOA. Each of these combinations individually computes the position of MT by exploiting the underlying geometric relations, subsequently averaging the results to mitigate the impact of noise. Therefore, the tracking performance of LKF can be improved. Combing (1) and (12), the classical LKF recursive algorithm for LOS propagation environment is given in Algorithm 2.

IV. The Proposed Tracking Algorithms with Only OB Path

In the OB scattering scenario, although the measured parameters shown in (3) are the nonlinear function of motion state $X(k)$, it is not possible to directly apply the existing algorithms, such as EKF or UKF, to track the position of MT. This is due to the fact that the position of the scatterer is unknown. In this section, we present two methods to cope with this problem. One is to derive the nonlinear relation between position of scatterer and the actual AOD/AOA, and the other one is to construct a new linear relation of the motion state $X(k)$ utilizing the geometric feature among the actual TOA/AOD/AOA.

A. The Tracking Algorithms based on Nonlinear Filtering

As shown in Fig. 2, the position of scatterer C is the interSection point of two lines. The equations of these two lines can be expressed as

$$\begin{aligned} y - y(k) &= tan(\alpha^0(k)) \cdot (x - x(k)) \\ y - y_1 &= tan(\beta^0(k)) \cdot (x - x_1), \end{aligned} \tag{18}$$

where tan is the function of tangent. Therefore, we can compute the position of scatterer as

$$\begin{aligned} x^{'}(k) &= \frac{a}{tan(\alpha^0(k)) - tan(\beta^0(k))}, \\ y^{'}(k) &= \frac{b}{tan(\alpha^0(k)) - tan(\beta^0(k))}, \end{aligned} \tag{19}$$

where $a = y_1 - tan(\beta^0(k)) \cdot x_1 + x(k) \cdot tan(\alpha^0(k)) - y(k)$, $b = tan(\alpha^0(k)) \cdot y_1 - tan(\alpha^0(k)) \cdot tan(\beta^0(k)) \cdot x_1 + tan(\alpha^0(k)) \cdot tan(\beta^0(k)) \cdot x(k) - tan(\beta^0(k)) \cdot y(k)$.

Substituting (19) into (3), we can obtain the nonlinear measurement as follows:

$$r(k) = h(X(k), m(k), v(k)) + n(k), \tag{20}$$

where

$$\begin{aligned} h(X(k), m(k), v(k)) =& \sqrt{(x(k) - x'(k))^2 + (y(k) - y'(k))^2} \\ &+ \sqrt{(x_1 - x'(k))^2 + (y_1 - y'(k))^2}, \end{aligned} \tag{21}$$

Following similar concepts of Taylor series, we can linearize this nonlinear measurement function around the predicted estimate $\hat{X}(k)$ using the partial derivatives of the measurement function as follows:

$$\begin{aligned} h(X(k), m(k), v(k)) =& h(\hat{X}(k), 0, 0) + H \cdot (X(k) - \hat{X}(k)) \\ &+ V \cdot \begin{pmatrix} m(k) \\ v(k) \end{pmatrix}, \end{aligned} \tag{22}$$

where

$$H = \left[\frac{\partial h}{\partial x(k)}(\hat{X}(k), 0, 0), \frac{\partial h}{\partial y(k)}(\hat{X}(k), 0, 0), 0, 0 \right], \tag{23}$$

$$\begin{aligned} \frac{\partial h}{\partial x(k)} =& \frac{(x^{'}(k) - x(k))(\frac{\partial x^{'}(k)}{\partial x(k)} - 1) + (y^{'}(k) - y(k))\frac{\partial y^{'}(k)}{\partial x(k)}}{\sqrt{(x^{'}(k) - x(k))^2 + (y^{'}(k) - y(k))^2}} \\ &+ \frac{(x^{'}(k) - x_1)\frac{\partial x^{'}(k)}{\partial x(k)} + (y^{'}(k) - y_1)\frac{\partial y^{'}(k)}{\partial x(k)}}{\sqrt{(x^{'}(k) - x_1)^2 + (y^{'}(k) - y_1)^2}}, \end{aligned}$$

$$\begin{aligned} \frac{\partial h}{\partial y(k)} =& \frac{(x^{'}(k) - x(k))\frac{\partial x^{'}(k)}{\partial y(k)} + (y^{'}(k) - y(k))(\frac{\partial y^{'}(k)}{\partial y(k)} - 1)}{\sqrt{(x^{'}(k) - x(k))^2 + (y^{'}(k) - y(k))^2}} \\ &+ \frac{(x^{'}(k) - x_1)\frac{\partial x^{'}(k)}{\partial y(k)} + (y^{'}(k) - y_1)\frac{\partial y^{'}(k)}{\partial y(k)}}{\sqrt{(x^{'}(k) - x_1)^2 + (y^{'}(k) - y_1)^2}}, \end{aligned}$$

$$\frac{\partial x^{'}(k)}{\partial x(k)} = \frac{tan(\alpha^0(k))}{tan(\alpha^0(k)) - tan(\beta^0(k))},$$

$$\frac{\partial x^{'}(k)}{\partial y(k)} = -\frac{1}{tan(\alpha^0(k)) - tan(\beta^0(k))},$$

$$\frac{\partial y^{'}(k)}{\partial x(k)} = \frac{tan(\alpha^0(k)) \cdot tan(\beta^0(k))}{tan(\alpha^0(k)) - tan(\beta^0(k))},$$

$$\frac{\partial y^{'}(k)}{\partial y(k)} = -\frac{tan(\beta^0(k))}{tan(\alpha^0(k)) - tan(\beta^0(k))},$$

$$V = \left[\frac{\partial h}{\partial m(k)}(\hat{X}(k), 0, 0), \frac{\partial h}{\partial v(k)}(\hat{X}(k), 0, 0), 0, 0 \right], \tag{24}$$

$$\begin{aligned} \frac{\partial h}{\partial m(k)} =& \frac{(x^{'}(k) - x(k))\frac{\partial x^{'}(k)}{\partial m(k)} + (y^{'}(k) - y(k))\frac{\partial y^{'}(k)}{\partial m(k)}}{\sqrt{(x^{'}(k) - x(k))^2 + (y^{'}(k) - y(k))^2}} \\ &+ \frac{(x^{'}(k) - x_1)\frac{\partial x^{'}(k)}{\partial m(k)} + (y^{'}(k) - y_1)\frac{\partial y^{'}(k)}{\partial m(k)}}{\sqrt{(x^{'}(k) - x_1)^2 + (y^{'}(k) - y_1)^2}}, \end{aligned}$$

$$\frac{\partial h}{\partial v(k)} = \frac{(x^{'}(k)-x(k))\frac{\partial x^{'}(k)}{\partial v(k)} + (y^{'}(k)-y(k))\frac{\partial y^{'}(k)}{\partial v(k)}}{\sqrt{(x^{'}(k)-x(k))^2+(y^{'}(k)-y(k))^2}} + \frac{(x^{'}(k)-x_1)\frac{\partial x^{'}(k)}{\partial v(k)} + (y^{'}(k)-y_1)\frac{\partial y^{'}(k)}{\partial v(k)}}{\sqrt{(x^{'}(k)-x_1)^2+(y^{'}(k)-y_1)^2}},$$

$$\frac{\partial x^{'}(k)}{\partial m(k)} = \frac{x(k)\cdot\frac{-(tan(\alpha^0(k))-tan(\beta^0(k)))}{cos^2(\alpha^0(k))} - \frac{-a}{cos^2(\alpha^0(k))}}{(tan(\alpha^0(k))-tan(\beta^0(k)))^2},$$

$$\frac{\partial y^{'}(k)}{\partial m(k)} = \frac{x_1\cdot\frac{tan(\alpha^0(k))-tan(\beta^0(k))}{cos^2(\alpha^0(k))} - \frac{a}{cos^2(\alpha^0(k))}}{(tan(\alpha^0(k))-tan(\beta^0(k)))^2},$$

$$\frac{\partial x^{'}(k)}{\partial v(k)} = \frac{d\cdot(tan(\alpha^0(k))-tan(\beta^0(k))) + b\cdot\frac{1}{cos^2(\alpha^0(k))}}{(tan(\alpha^0(k))-tan(\beta^0(k))^2},$$

$$\frac{\partial y^{'}(k)}{\partial v(k)} = \frac{e\cdot(tan(\alpha^0(k))-tan(\beta^0(k))) - b\cdot\frac{1}{cos^2(\beta^0(k))}}{(tan(\alpha^0(k))-tan(\beta^0(k)))^2},$$

$$d = -y_1\cdot\frac{1}{cos^2(\alpha^0(k))} + (x_1-x(k))\cdot tan(\beta^0(k))\cdot\frac{1}{cos^2(\alpha^0(k))},$$

$$e = (x_1-x(k))\cdot tan(\alpha^0(k))\cdot\frac{1}{cos^2(\beta^0(k))} + y(k)\cdot\frac{1}{cos^2(\beta^0(k))}.$$

Substituting (22) into (20), we obtain the approximated range as follows:

$$r(k) = h(\hat{X}(k),0,0) + H\cdot(X(k)-\hat{X}(k)) + V\cdot\begin{pmatrix} m(k) \\ v(k)\end{pmatrix} + n(k). \tag{25}$$

Thus, the EKF recursive algorithm for OB scattering environment is summarized in Algorithm 3.

As we know, EKF linearizes the nonlinear system model by Taylor series expansion and assumes that the noise is Gaussian distribution. From (20), due to the unknown scatterer whose position is computed from (19), it is highly nonlinear relation with the position of MT. In addition, the noise in (20) is non-Gaussian. Therefore, EKF may lead to large errors in OB scattering environment. Different to EKF, the UKF approximates the probability distribution of nonlinear functions through the unscented transform, a process that does not entirely rely on the assumption of Gaussian noise. The UKF selects a specific set of points known as sigma points, which can represent the Gaussian distribution of the original state. These points are then transformed through the nonlinear function, yielding an approximation of the probability distribution of the transformed state. This method can preserve the characteristics of nonlinear functions more accurately, thereby providing good performance even when dealing with nonlinear Gaussian noise [43], [44]. Furthermore, in our tracking problem, the state model of (1) is linear and Gaussian, whereas the measurement model of (20) is nonlinear and non-Gaussian. This scenario can be effectively handled by the UKF [44], and the utilization of particle filters is advocated in scenarios for which the models are entirely nonlinear and non-Gaussian.

Algorithm 3 OB-EKF

1: Initialization: $k=0$, set the state vector $X(0)$ and the covariance $P(0)$;
2: Recursive estimation: For $k=1,2,\cdots$
3: Time update: Project the state vector and covariance ahead from (1), $\hat{X}(k)=A\cdot X(k-1)$, $\hat{P}(k)=A\cdot P(k-1)\cdot A^T+G\cdot Q\cdot G^T$;
4: Measurement update: Compute the position of scatterer with $\hat{X}(k)$ according to (19);
5: Compute the linear vector H and V according to (23) and (24).
6: Compute the variance of measurement noise in (25), $R = V\cdot\begin{bmatrix}\sigma_\alpha^2 & 0\\ 0 & \sigma_\beta^2\end{bmatrix}\cdot V^H+\sigma_n^2$;
7: Calculate the Kalman gain $K=\hat{P}(k)\cdot H^T\cdot(H\cdot\hat{P}(k)\cdot H^T+R)^{-1}$;
8: Update the state vector and covariance estimate with measurement $r(k)$ shown in (21) and (25), $X(k)=\hat{X}(k)+K\cdot(r(k)-h(\hat{X}(k),0,0))$, $P(k)=\hat{P}(k)-K\cdot H\cdot\hat{P}(k)$;

Since the state vector can be predicted from (1), we can directly generate the sigma points in the UKF through unscented transform

$$\chi^i(k) = \begin{cases} \hat{X}^{'}(k), & i=0 \\ \hat{X}^{'}(k)+\left(\sqrt{(M+\lambda)\hat{P}^{'}(k)}\right)^i, & i=1,\cdots,M \\ \hat{X}^{'}(k)-\left(\sqrt{(M+\lambda)\hat{P}^{'}(k)}\right)^i, & i=M+1,\cdots,2M \end{cases} \tag{26}$$

where M is the dimension of vector $\hat{X}^{'}(k)$, $\lambda=\alpha^2(M+\kappa)-M$ is a scaling parameter, α is a parameter that determines the spread of the sigma points and is usually set to a small positive value (for example, 1e-3), κ is a secondary scaling parameter which is usually set to 0, $(\sqrt{(M+\lambda)\hat{P}^{'}(k)})^i$ is the ith row of the matrix square root X which is satisfied with $X\cdot X=(M+\lambda)\hat{P}^{'}(k)$, where

$$\hat{X}^{'}(k) = \begin{bmatrix}\hat{X}(k)\\ 0\\ 0\end{bmatrix}_{M\times 1},$$

$$\hat{P}^{'}(k) = \begin{bmatrix}\hat{P}^(k) & 0_{4\times1} & 0_{4\times1} & 0_{4\times1}\\ 0_{1\times4} & \sigma_n^2 & 0 & 0\\ 0_{1\times4} & 0 & \sigma_\alpha^2 & 0\\ 0_{1\times4} & 0 & 0 & \sigma_\beta^2\end{bmatrix},$$

$0_{m\times n}$ is a m-by-n matrix of zeros.

Algorithm 4 OB-UKF

1: Initialization: $k = 0$, set the state vector $X(0)$ and the covariance $P(0)$;
2: Recursive estimation: For $k = 1, 2, \cdots$
3: Time update: Project the state vector and covariance ahead from (1), $\hat{X}(k) = A \cdot X(k-1)$, $\hat{P}(k) = A \cdot P(k-1) \cdot A^T + G \cdot Q \cdot G^T$;
4: Measurement update: Generate the sigma points with $\hat{X}(k)$ and $\hat{P}(k)$, and the corresponding weights according to (26) and (27);
5: For each sigma point $\chi^i(k)$, compute the position of scatterer and the estimated range $h(\chi^i(k))$ according to (19) and (21);
6: Compute the estimated mean and variance of range measurement, and then the covariance of state vector and range measurement $\mu_r(k) = \sum_{i=0}^{2M} Wm^i \cdot h(\chi^i(k))$, $P_{rr}(k) = \sum_{i=0}^{2M} Wc^i \cdot (h(\chi^i(k)) - \mu_r(k)) \cdot (h(\chi^i(k)) - \mu_r(k))^T$, $P_{Xr}(k) = \sum_{i=0}^{2M} Wc^i \cdot (\chi^i(k)_{1:4} - \hat{X}(k)) \cdot (h(\chi^i(k)) - \mu_r(k))^T$, where $\chi^i(k)_{1:4}$ denotes the four dimensional vector whose value is the same as the first four elements of $\chi^i(k)$;
7: Calculate the Kalman gain $K = P_{Xr}(k) \cdot P_{rr}(k)^{-1}$;
8: Update the state vector and covariance estimate $X(k) = \hat{X}(k) + K \cdot (r(k) - \mu_r(k))$, $P(k) = \hat{P}(k) - K \cdot P_{Xr}(k)^T$;

The corresponding weights of sigma points are defined as

$$Wm^i = \begin{cases} \frac{\lambda}{M+\lambda}, & i = 0 \\ \frac{1}{2(M+\lambda)}, & i \neq 0 \end{cases},$$
$$Wc^i = \begin{cases} \frac{\lambda}{M+\lambda} + 1 - \alpha^2 + \beta, & i = 0 \\ \frac{1}{2(M+\lambda)}, & i \neq 0 \end{cases}, \tag{27}$$

where β is used to incorporate prior knowledge of the distribution ($\beta = 2$ is optimal for Gaussian distribution). Wm^i and Wc^i are used to compute the mean and covariance of the posterior sigma points, respectively.

Based on the above explanation, the UKF recursive algorithm for OB scattering environment is summarized in Algorithm 4.

B. The Tracking Algorithm based on Linear Filtering

From (3), it is obvious that the nonlinear filter can be used to deal with this tracking problem. However, when signal experiences OB scattering, as shown in Fig. 2, the position of MT is on the line of AB if the measured noise is ignored. Thus, the true nonlinear measured parameters in (3) can be transformed into the following linear form:

$$\begin{aligned} &\big(cos(\alpha^0(k)) + cos(\beta^0(k))\big) \cdot y(k) \\ &- \big(sin(\alpha^0(k)) + sin(\beta^0(k))\big) \cdot x(k) \\ &= y_1 \cdot \big(cos(\alpha^0(k)) + cos(\beta^0(k))\big) \\ &\quad - x_1 \cdot \big(sin(\alpha^0(k)) + sin(\beta^0(k))\big) \\ &\quad - r^0(k) \cdot sin(\alpha^0(k) - \beta^0(k)). \end{aligned} \tag{28}$$

When substituting the measured parameters in (3) into (28), to obtain the simple results, a reasonable approximation about trigonometric function of actual angles can be given as follows:

$$\begin{aligned} cos(\alpha^0(k)) + cos(\beta^0(k)) \approx& cos(\alpha(k)) + cos(\beta(k)) \\ sin(\alpha^0(k)) + sin(\beta^0(k)) \approx& sin(\alpha(k)) + sin(\beta(k)) \\ sin(\alpha^0(k) - \beta^0(k)) \approx& sin(\alpha(k) - \beta(k)) - cos(\alpha(k) \\ & - \beta(k)) \cdot (m(k) - v(k)). \end{aligned} \tag{29}$$

Then, we can obtain the following approximation equation in matrix form:

$$Y(k) = H(k) \cdot X(k) + \varepsilon(k), \tag{30}$$

where

$$\begin{aligned} Y(k) =& y_1 \cdot (cos(\alpha(k)) + cos(\beta(k))) - x_1 \cdot (sin(\alpha(k)) \\ &+ sin(\beta(k))) - r(k) \cdot sin(\alpha(k) - \beta(k)), \end{aligned} \tag{31}$$

$$\begin{aligned} &H(k) = \\ &[-sin(\alpha(k)) - sin(\beta(k)), cos(\alpha(k)) + cos(\beta(k)), 0, 0], \end{aligned} \tag{32}$$

$$\begin{aligned} \varepsilon(k) =& r(k) \cdot cos(\alpha(k) - \beta(k)) \cdot (m(k) - v(k)) + sin(\alpha(k) \\ &- \beta(k)) \cdot n(k) - cos(\alpha(k) - \beta(k)) \cdot n(k) \cdot m(k) \\ &+ cos(\alpha(k) - \beta(k)) \cdot n(k) \cdot v(k). \end{aligned} \tag{33}$$

From (33), the noise $\varepsilon(k)$ contains not only additive noise, but also multiplicative noise, but it can be approximated as a Gaussian distribution. Combining (1) with (30), the classical LKF recursive algorithm for OB scattering environment is provided in Algorithm 5.

Algorithm 5 OB-LKF

1: Initialization: $k = 0$, set the state vector $X(0)$ and the covariance $P(0)$;
2: Recursive estimation: For $k = 1, 2, \cdots$
3: Time update: Project the state vector and covariance ahead from (1), $\hat{X}(k) = A \cdot X(k-1)$, $\hat{P}(k) = A \cdot P(k-1) \cdot A^T + G \cdot Q \cdot G^T$;
4: Measurement update: Compute linear matrix $H(k)$ and new measurement $Y(k)$ according to (31) and (32);
5: Compute the variance of $\varepsilon(k)$ according to (33), $R = r^2(k) cos^2(\alpha(k) - \beta(k))(\sigma_\alpha^2 + \sigma_\beta^2) + sin^2(\alpha(k) - \beta(k))\sigma_n^2 + cos^2(\alpha(k) - \beta(k))(\sigma_\alpha^2 + \sigma_\beta^2)\sigma_n^2$;
6: Calculate the Kalman gain $K = \hat{P}(k) \cdot H(k)^T \cdot (H(k) \cdot \hat{P}(k) \cdot H(k)^T + R)^{-1}$;
7: Update the state vector and covariance estimate, $X(k) = \hat{X}(k) + K \cdot (Y(k) - H(k) \cdot \hat{X}(k))$, $P(k) = \hat{P}(k) - K \cdot H(k) \cdot \hat{P}(k)$;

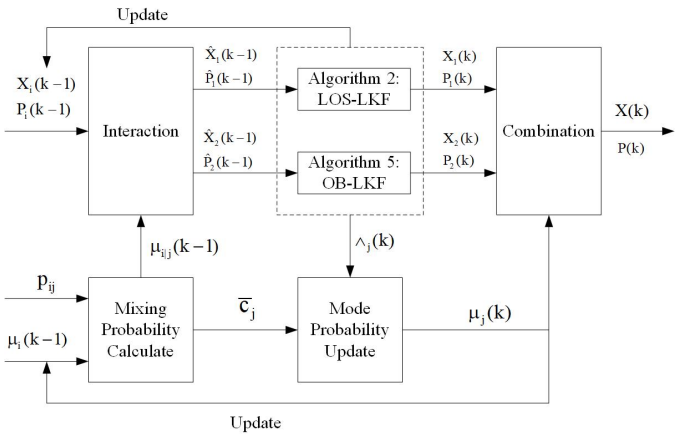

Fig. 3. The architecture of IMM algorithm.

V. The Proposed Tracking Algorithms with Hybrid LOS and OB Path

The above analysis assume that all the propagation paths are LOS or OB scattering. However, the LOS and OB scattering shown in Fig. 1 may appear alternatively. Thus, when both LOS and OB scattering paths are present, the proposed EKF, UKF or LKF algorithms shown in Section III and IV are not adaptable. Therefore, new methods need to be developed to deal with this scenario. Our idea is developed based on two aspects. On the one hand, the propagation path LOS or OB scattering is considered to be a Markov process with two interactive modes named as IMM. On the other hand, LOS or OB scattering is identified first, and then the corresponding filtering algorithm is applied to it.

A. Modified IMM LKF Tracking Algorithm

The signal propagation between the BS and the MT with LOS or OB scattering can be considered as a switching mode system and a two-state Markov process can describe this switching mode system. Thus, based on the basic principle of IMM algorithm [6], [8], [11], [18], [22], we can directly track the position of MT with our proposed LOS-LKF and OB-LKF algorithms. This algorithm illustrated in Fig.3 is consists of five parts, the mixing probability, the interaction, the LKF algorithm, the mode probability update and the combination. The state is estimated by two parallel LKF algorithms (i.e., Algorithm 2: LOS-LKF and Algorithm 5: OB-LKF) based on the corresponding models.

In [6], [11], [22], the mode probabilities of the present conditions are calculated and updated by a likelihood function via their respective estimate errors. However, the likelihood function in LOS-LKF is not suitable. The error of (12) in LOS-LKF is a two-dimensional vector, its likelihood function needs to compute the covariance matrix of errors. After a few iterations, the probability of LOS is almost zero, which lead to the performance degradation of tracking. Therefore, we need to find another likelihood function to adapt the LOS-LKF mode. Fortunately, in LOS propagation, we can use the estimate error of range measurement to evaluate the tracking accuracy of MT rather than the estimate error of (12). Thus, the modified IMM-LKF recursive algorithm referred to as M-IMM-LKF is proposed and summarized in Algorithm 6.

Algorithm 6 Modified IMM-LKF (M-IMM-LKF)

1: Initialization: $k = 0$, Set the initial mean and covariance of two LKF algorithms $X_i(0)$, $P_i(0)$, $i = 1, 2$, the prior probabilities $\mu_i(0), i = 1, 2$, and the transition probability matrix $T = \begin{bmatrix} p_{11} & p_{12} \\ p_{21} & p_{22} \end{bmatrix}$;
2: Recursive estimation: For $k = 1, 2, \cdots$
3: Mixing probability calculation $i, j = 1, 2$, $\mu_{i|j}(k-1) = (1/\tilde{c}_j)p_{ij}\mu_j(k-1)$, $\tilde{c}_j = \sum_{i=1}^{2} p_{ij}\mu_i(k-1)$;
4: Interaction $j = 1, 2$ $\hat{X}_j(k-1) = \sum_{i=1}^{2} X_i(k-1)\cdot\mu_{i|j}(k-1)$, $\hat{P}_j(k-1) = \sum_{i=1}^{2} \mu_{i|j}(k-1)\cdot(P_i(k-1) + (X_i(k-1) - \hat{X}_j(k-1))\cdot(X_i(k-1) - \hat{X}_j(k-1))^T)$;
5: Two LKF algorithms: LOS-LKF shown in Algorithm 3 outputs the mean $X_1(k)$ and covariance $P_1(k)$, then use $X_1(k)$ to compute the estimated range $\hat{r}(k)$ from (2). Thus, the error is $e_1(k) = r(k) - \hat{r}(k)$ and variance $W_1(k) = \sigma_n^2$. Then, the likelihood function of LOS propagation is $\bigwedge_1(k) = N(e_1(k); 0, W_1(k))$. OB-LKF shown in Algorithm 6 also outputs the mean $X_2(k)$ and covariance $P_2(k)$, then compute the error $e_2(k) = Y(k) - H(k)\cdot\hat{X}_2(k)$ and variance $W_2(k) = H(k)\cdot\hat{P}(k)\cdot H(k)^T + R$, then the likelihood function of OB scattering propagation is $\bigwedge_2(k) = N(e_2(k); 0, W_2(k))$;
6: Mode probability update: $j = 1, 2$, $\mu_j(k) = \frac{1}{c}\bigwedge_j(k)\cdot\tilde{c}_j$, $c = \sum_{j=1}^{2}\bigwedge_j(k)\cdot\tilde{c}_j$;
7: Combination $X(k) = \sum_{j=1}^{2} X_j(k)\cdot\mu_j(k)$, $P(k) = \sum_{j=1}^{2}\mu_j(k)\cdot(P_j(k) + (X_j(k) - X(k))\cdot(X_j(k) - X(k))^T)$;

Algorithm 7 I-LKF

1: Initialization: $k = 0$, Set the state vector $X(0)$, the covariance $P(0)$, and the probability of detection P_d;
2: Recursive estimation: For $k = 1, 2, \cdots$
3: Compute the threshold Δ from (35) with the known standard deviation of angle measurement σ_α and σ_β;
4: Determine whether the AOD and AOA measurement is satisfied with (34);
5: If it is satisfied, LOS-LKF shown in Algorithm 2 outputs the updated state vector $X(k)$ and covariance $P(k)$;
6: Otherwise, OB-LKF shown in Algorithm 5 outputs the updated state vector $X(k)$ and covariance $P(k)$;

B. LKF Tracking Algorithm based on LOS Identification

Without the knowledge of signal propagation condition, the idea of IMM algorithm is to model it as a two-state Markov process. However, if the condition of signal propagation can be identified correctly, we can then apply the corresponding LOS or OB LKF algorithm to track the position of MT. The work in [31] introduces a small positive number Δ as a threshold

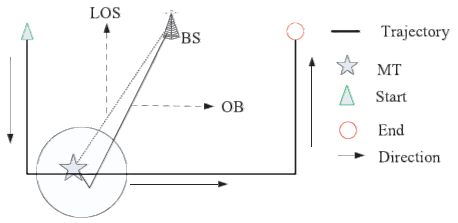

Fig. 4. Simulation scenario in a wireless network.

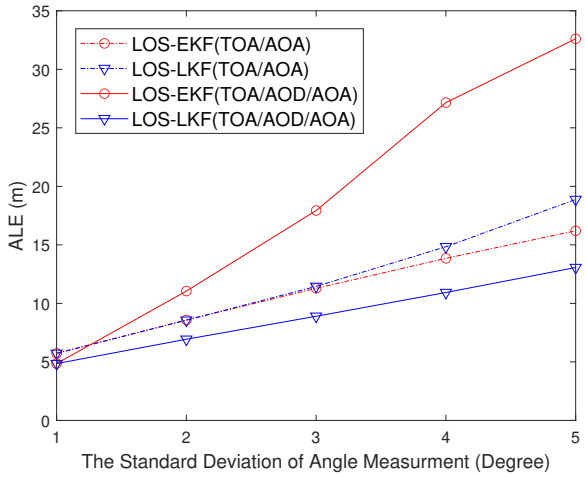

Fig. 5. ALE versus the standard deviation of angle measurement in LOS environment.

to identify LOS propagation when it satisfies the following condition:

$$\pi - \Delta \leq |\alpha(k) - \beta(k)| \leq \pi + \Delta. \tag{34}$$

Furthermore, this threshold Δ is determined by the probability of detection P_d as

$$1 - 2 \cdot Q(\frac{\Delta}{\sqrt{\sigma_\alpha^2 + \sigma_\beta^2}}) = P_d, \tag{35}$$

where $Q(x) = (1/\sqrt{2\pi}) \int_x^\infty e^{-t^2/2} dt$.

Then, the identified LKF recursive algorithm with linear state model (1) and linear measurement model (12) or (30) denoted as I-LKF is presented in Algorithm 7.

VI. Simulation Results and Discussion

In this section, we provide simulation results to validate the proposed tracking algorithms and compare the localization accuracy of MT tracking under different propagation environments. The MT has a steady velocity of 10 m/s and moves in a trajectory as shown in Fig. 4. The sample length and the sample interval Δt are 200 and 1 s, respectively. The position of BS is $(0, 0)$ and the random acceleration variance σ_w^2 shown in (1) is chosen as 1 m/s^2. The angle measurement noise shown in (2) and (3) is assumed to

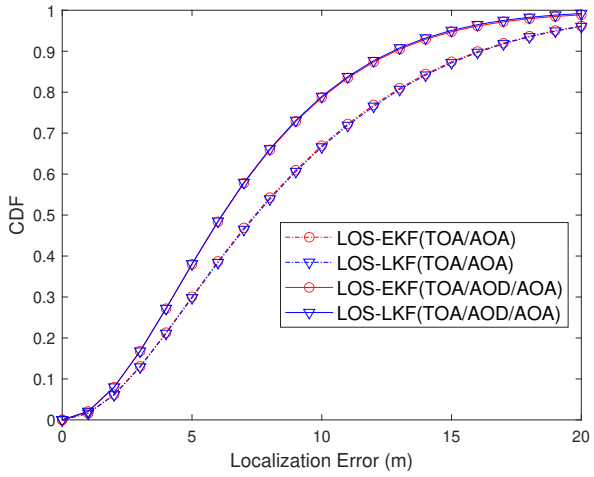

Fig. 6. CDF of localization error in LOS environment.

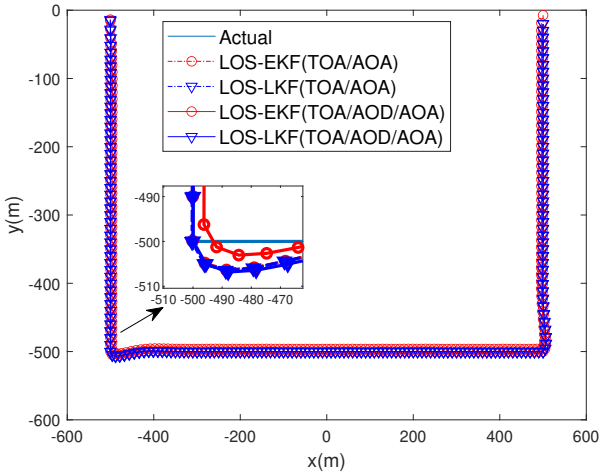

Fig. 7. ALE versus time instant in LOS environment.

be a white Gaussian random variable with zero mean and the same standard deviation $\sigma_\alpha = \sigma_\beta$, whereas the range measurement noise is also assumed to be a white random variable with zero mean and standard deviation $\sigma_n = 5$ m. The initial estimate of MT is $X(0) = [-500, 0, 0, -10]^T$ with initial covariance matrix $P(0) = diag[100, 100, 100, 100]$. In order to compare the estimated trajectory and cumulative probability distribution (CDF) of localization error with different algorithms, root square error (RSE) defined as $RSE = \sqrt{(\hat{x}(k) - x(k))^2 + (\hat{y}(k) - y(k))^2}$ is chosen as the criterion. Moreover, in order to smooth the effect of measured noise at time k, the corresponding average localization error (ALE) defined as $ALE = (1/N) \sum_{i=1}^{N} \sqrt{(\hat{x}_i(k) - x(k))^2 + (\hat{y}_i(k) - y(k))^2}$, where $N = 500$ is the number of Monte-Carlo simulations.

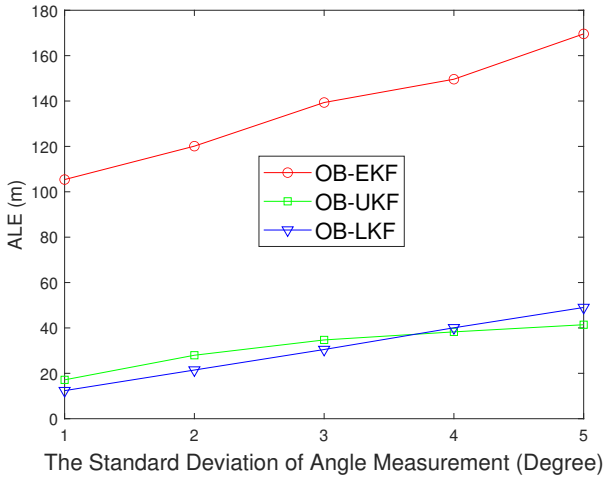

Fig. 8. ALE versus the standard deviation of angle measurement in OB scattering environment.

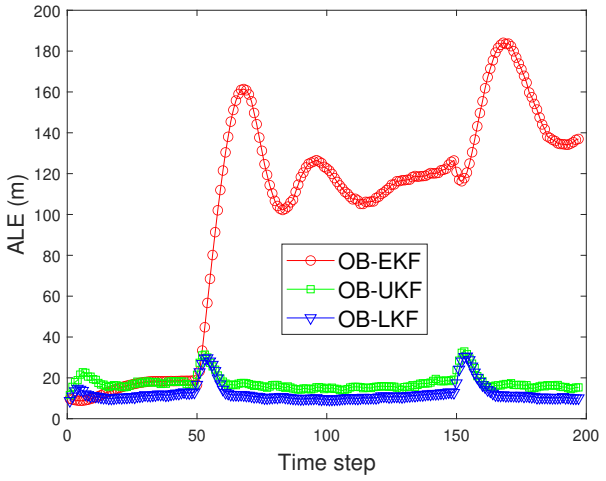

Fig. 9. The estimated and actual trajectories of MT in OB scattering environment.

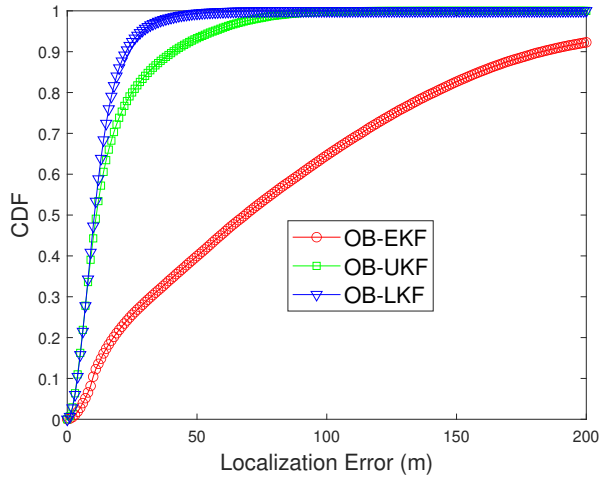

Fig. 10. CDF of localization error in OB scattering environment.

A. Simulation of LOS or OB Scattering Environment

1) Simulation of LOS environment: For LOS scenario, the range and angle measurement parameters are generated from (2). We have evaluated and compared two algorithms, i.e., LOS-EKF and LOS-LKF, each with and without AOD measurements. Due to significant effect of the angle error, Fig. 5 shows the ALE versus the standard deviation of angle measurement. When the angle error is small, all the algorithms have the similar performance. However, as the increase of the angle error, the performance of all algorithms is degraded. Notably, our proposed LOS-LKF with TOA/AOD/AOA performs the best tracking accuracy. Interestingly, it is observed that the inclusion of AOD measurement in EKF does not enhance but rather diminishes its tracking accuracy. The reason is that the AOD is highly correlated with the AOA, and the non-diagonal elements of the covariance matrix will be significantly non-zero. This affects the calculation of Kalman gain, resulting in a decrease in tracking accuracy. The standard deviation of angle measurement is set to 2°, the ALE versus time instant k is presented in Fig. **??**, and the CDF of localization error is shown in Fig. 6. In addition, Fig. 7 illustrates the estimated and actual trajectories of MT. From Figs. **??**–7, we realize that the tracking accuracy of our proposed LOS-LKF is the best, and comparatively large localization errors are occurred when the motion direction of MT is changed.

2) Simulation of OB scattering environment: In OB scattering environment, the range and angle measurement parameters are generated from (3). The position of scatterer is located inside a circular disk of fixed radius R_d, which is called the circular scattering model [25], [30], [31], [32], [45], [46] whose distance from a scatterer to MT is uniformly distributed in the range of $[0, R_d]$, and the angle is uniformly distributed in the range of $[0, 2\pi]$. Three algorithms, i.e., OB-EKF, OB-UKF, and OB-LKF are evaluated and compared. Our proposed OB-LKF assumes that the angle error is small. In order to validate the effectiveness of it with large angle error, Fig. 8 illustrates the ALE versus the standard deviation of angle measurement. It is shown that both OB-LKF and OB-UKF are better than OB-EKF. As the increase of the angle error, the performance of two algorithms is degraded. When the angle error is small, OB-LKF is slightly superior to OB-UKF. As the increase of the angle error whose value is larger than four degrees, OB-LKF is slightly worse than OB-UKF. In addition, the standard deviation of angle measurement is set to 1°, Fig. 9 presents the estimated and actual trajectories of MT, the CDF of localization error is shown in Fig. 10, and the ALE versus time instant k is presented in Fig. 11. From Figs. 9–11, it is easy to see that, most of the time, the OB-LKF has the highest localization accuracy, followed by OB-UKF and then OB-EKF. The OB-LKF and OB-UKF can track the trajectory of MT very well, whereas the tracking accuracy of OB-EKF is decreased as time goes by. The reason is that EKF algorithm with first-order Taylor series expansion is not effective for highly nonlinear problems. As the same conclusion in LOS environment, comparatively large localization errors also occur

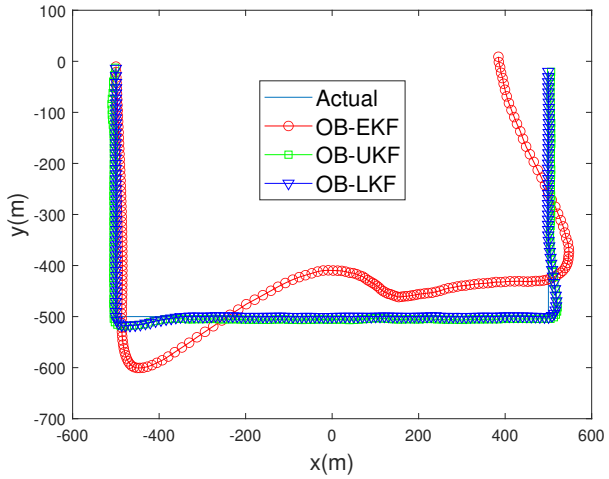

Fig. 11. ALE versus time instant in OB scattering environment.

TABLE I
COMPUTER RUNNING TIME OF THREE ALGORITHMS.

Methods		UKF	EKF	LKF
Computer running time	LOS	-	0.026 ms	0.021 ms
	OB scattering	0.077 ms	0.013 ms	0.010 ms

when the motion direction of MT is changed.

3) Comparison of running time: From the literature, the computational complexity of EKF, UKF, and LKF can be easily understood. UKF is the highest, followed by EKF and then LKF. However, the comparison of the actual computational time about these three algorithms is more convincing. Table I provides the computational time of three algorithms with an average of 10000 runs. The experiments are processed on the computer with Intel ® Core™ i5-6200U CPU 64 bit processor and 4 GB memory. From Table I, it can be realized that the computer running time of LKF is the lowest, while that of UKF is the highest. These results confirm our knowledge on this. However, it is seen that the running time of these three algorithms in OB scattering is more than that of LOS. In fact, the updated stage of UKF and EKF need to compute the estimated range and angles in LOS, whereas only the estimated range is computed in OB scattering. In addition, there are two measurement equations in LOS, while only one is existing in OB scattering. Therefore, it is reasonable that the running time of LOS is higher than that of OB scattering.

In this subsection, three algorithms, i.e., EKF, UKF and LKF, are compared with hybrid TOA/AOD/AOA measurements in LOS or OB scattering condition. From the simulation results, in any of these conditions, the proposed LKF algorithm can track the position of MT accurately. Moreover, the comparison of running time demonstrates that LKF algorithm has also the lowest computational time. Therefore, our proposed LKF algorithms are better methods to track the position of MT in their respective conditions.

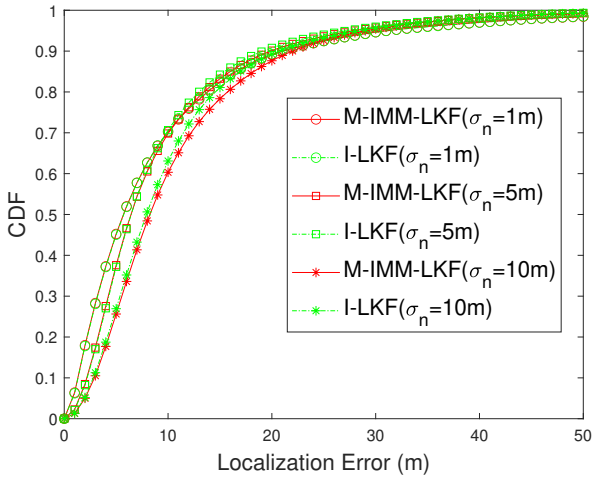

Fig. 12. The CDF of localization error with different range measurement standard deviation.

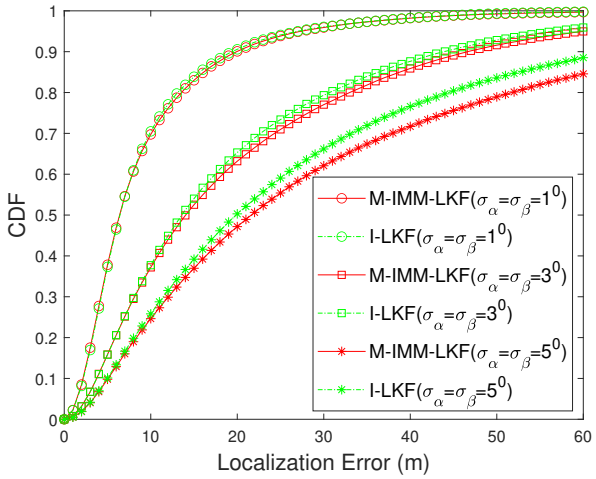

Fig. 13. The CDF of localization error with different angle measurement standard deviation.

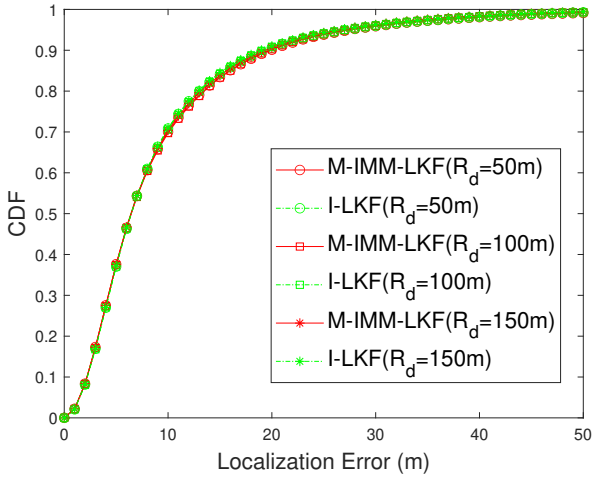

Fig. 14. The CDF of localization error with different scattering radius.

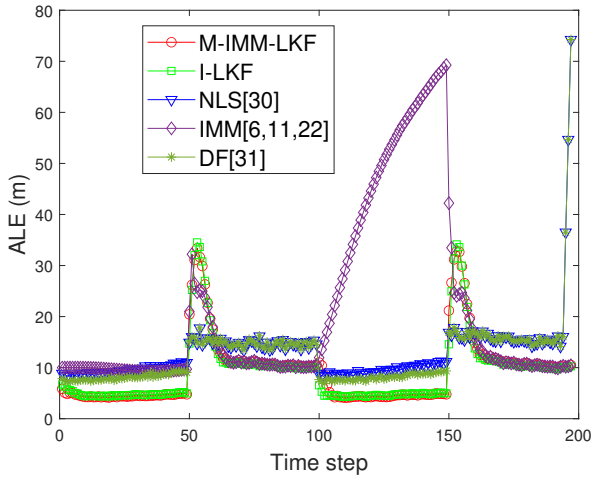

Fig. 15. The estimated and actual trajectories of MT in hybrid LOS and OB scattering environment.

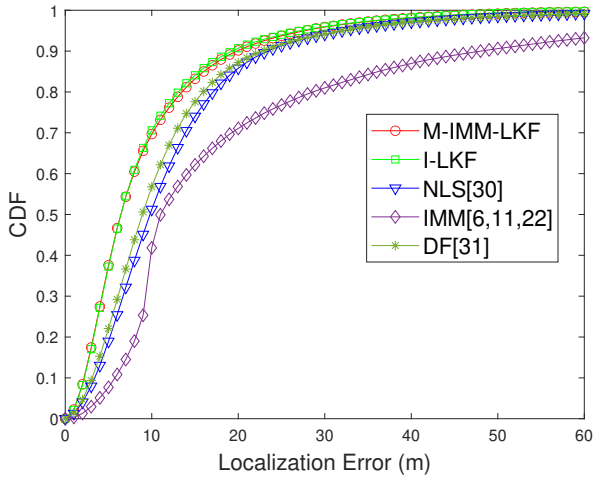

Fig. 16. CDF of localization error in hybrid LOS and OB scattering environment.

B. Simulation of Hybrid LOS and OB Scattering Environment

In our simulation, LOS or OB scattering is changed for each 50 samples in an alternate way. The measured range and angle are generated using the same method mentioned in Section A. The two-state Markov transition probability matrix for the M-IMM-LKF algorithm is chosen by $T = \begin{bmatrix} p_{11} & p_{12} \\ p_{21} & p_{22} \end{bmatrix} = \begin{bmatrix} 0.95 & 0.05 \\ 0.05 & 0.95 \end{bmatrix}$, and the initial prior probabilities are set to $\mu_i = 0.5$, $i = 1, 2$. The probability of detection for I-LKF is set to $P_d = 0.95$.

1) Analysis of the proposed tracking algorithms: The performance of the proposed tracking algorithms are affected by three factors, i.e., the range standard deviation σ_n, angle standard deviation σ_α, σ_β, and scattering radius R_d. Fig. 12 provides the CDF of localization error with different σ_n. When σ_n is small, the proposed two algorithms have the same performance. As it increases, I-LKF is slightly better than M-IMM-LKF. As shown in Fig. 13, we see that σ_α, σ_β has greater influence on our proposed algorithms than σ_n. As the increase of σ_α, σ_β, the performance is greatly reduced. But, I-LKF is still superior to M-IMM-LKF . From Fig. 14, it is shown that R_d has little effect on our proposed algorithms.

2) Comparison with the existing algorithms: Due to the one propagation path with TOA/AOD/AOA measurement, only three other algorithms, i.e., NLS [30], IMM [6,11,22], and DF [31] can be compared. In hybrid LOS and OB scattering environment, Fig. 15 provides the estimated and actual trajectories of MT, the CDF of localization error is shown in Fig. 16, and the ALE versus time instant k is presented in Fig. 17. From Figs. 15–17, we see that IMM algorithm is not capable of tracking the position of MT accurately, and the proposed two algorithms are better than NLS and DF. When the motion direction of MT is changed and the

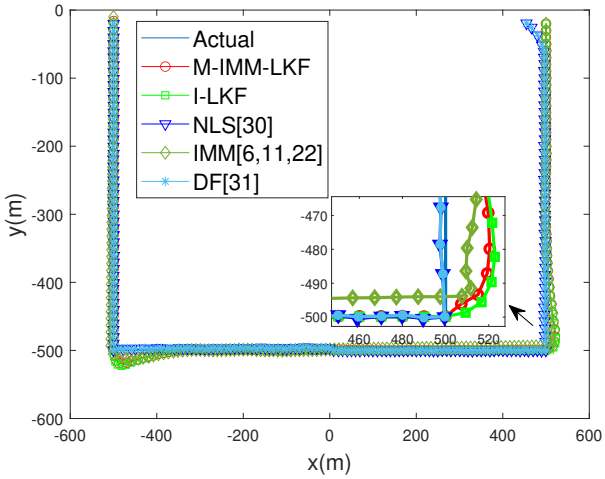

Fig. 17. ALE versus time instant in hybrid LOS and OB scattering environment.

LOS/OB scattering transition is happened, large localization error is present for our proposed algorithms. The reason is the inaccurate state estimation, and this state needs to be updated by the TOA/AOD/AOA measurement. After several iterations, the tracking accuracy is significantly improved. However, the localization errors of NLS and DF are relatively small, because these two algorithms do not rely on the state equation, and directly localize the MT with TOA/AOD/AOA measurements. Overall, the proposed algorithms are superior to the existing algorithms. In addition, from Algorithm 6 and Algorithm 7, it is obvious that the computational complexity of I-LKF is lower than that of IMM-LKF, and it is not necessary to compare the actual computational time of these two algorithms. Therefore, for hybrid TOA/AOA/AOD localization model, both M-IMM-LKF and I-LKF algorithm can deal with the problem about the frequent transition between LOS and OB scattering.

VII. Conclusions

In this paper, hybrid TOA/AOD/AOA tracking algorithms with single BS and one path were investigated in different propagation environments. In LOS propagation environment, the proposed LKF algorithm had the same localization accuracy with the existing EKF and UKF algorithms, but lower computational time. Moreover, in OB scattering environment, the performance of the proposed EKF, UKF, and LKF algorithms were evaluated and compared. Simulation results and running time analysis showed that LKF algorithm was superior to EKF and UKF algorithms. Finally, practical condition suffered from frequent transition between LOS and OB scattering was examined, two algorithms referred to as M-IMM-LKF and I-LKF were proposed to deal with the large localization error when the transition between the LOS and OB scattering occurred. it was also demonstrated that the proposed algorithms could remarkably reduce these localization errors.

References

[1] A. H. Sayed, A. Tarighat, and N. Khajehnouri, "Network-based wireless location: Challenges faced in developing techniques for accurate wireless location information," *IEEE Signal Process. Mag.*, vol. 22, no. 4, pp. 24–40, Jul. 2005.

[2] S. Wu, J. Li, and S. Liu, "Improved localization algorithms based on reference selection of linear least squares in LOS and NLOS environments," *Wireless Personal Commun.*, vol. 68, no. 1, pp. 187–200, Jan. 2013.

[3] C. Laoudias *et al.*, "A survey of enabling technologies for network localization, tracking, and navigation," *IEEE Commun. Surveys Tut.*, vol. 20, no. 4, pp. 3607–3644, Jul. 2018.

[4] J. Huang, J. Liang, and S. Luo, "Method and analysis of TOA-based localization in 5G ultra-dense networks with randomly distributed nodes," *IEEE Access*, vol. 7, pp. 174 986–175 002, Dec. 2019.

[5] D. Gaglione *et al.*, "Classification-aided multitarget tracking using the sum-product algorithm," *IEEE Signal Process. Lett.*, vol. 27, pp. 1710–1714, Sep. 2020.

[6] J. F. Liao and B. S. Chen, "Robust mobile location estimator with NLOS mitigation using interacting multiple model algorithm," *IEEE Trans. Wireless Commun.*, vol. 5, no. 11, pp. 3002–3006, Dec. 2006.

[7] C. Rohrig and M. Muller, "Indoor location tracking in non-line-of-sight environments using a IEEE 802.15.4a wireless network," in *Proc. IEEE/RSJ IROS*, 2009.

[8] L. Chen and L. Wu, "Mobile localization with NLOS mitigation using improved Rao-Blackwellized particle filtering algorithm," in *Proc. IEEE ISCE*, 2009.

[9] L. Chen and L. Wu, "Mobile positioning in mixed LOS/NLOS conditions using modifled EKF banks and data fusion method," *IEICE Trans. Commun.*, vol. 92-B, no. 1, pp. 1318–1325, Jan. 2009.

[10] L. Chen and R. Piche, "Mobile tracking and parameter learning in unknown non-line-of-sight conditions," in *Proc. IEEE FUSION*, 2010.

[11] U. Hammes and A. M. Zoubir, "Robust mt tracking based on m-estimation and interacting multiple model algorithm," *IEEE Trans. Signal Process.*, vol. 59, no. 7, pp. 3398–3409, Jul. 2011.

[12] X. Zhou, A. Jin, and Q. Meng, "NLOS error mitigation in mobile location based on modified extended Kalman filter," in *Proc. IEEE WCNC*, 2012.

[13] M. Ulmschneider and C. Gentner, "Multipath assisted positioning for pedestrians using LTE signals," in *Proc. IEEE/ION PLANS*, 2016.

[14] R. M. Vaghefi and R. M. Buehrer, "Cooperative source node tracking in non-line-of-sight environments," *IEEE Trans. Mobile Comput.*, vol. 16, no. 5, pp. 1287–1299, May. 2017.

[15] J. M. Pak, C. K. Ahn, and P. Shi, "Distributed hybrid particle/fir filtering for mitigating NLOS effects in TOA based localization using wireless sensor networks," *IEEE Trans. Ind. Electron.*, vol. 64, no. 6, pp. 5182–5191, Jan. 2017.

[16] H. Zhang and S. Y. Tan, "TOA based indoor localization and tracking via single-cluster PHD filtering," in *Proc. IEEE GLOBECOM*, 2017.

[17] Y. Zhao, X. Li, Y. Wang, and C. Z. Xu, "Biased constrained hybrid Kalman filter for range-based indoor localization," *IEEE Sensors J.*, vol. 18, no. 4, pp. 1647–1655, Feb. 2018.

[18] W. Cui, B. Li, L. Zhang, and W. Meng, "Robust mobile location estimation in NLOS environment using GMM, IMM, and EKF," *IEEE Systems J.*, vol. 13, no. 3, pp. 3490–3500, Sep. 2019.

[19] L. Cheng, H. Zhang, D. Wei, and J. Zhou, "An indoor tracking algorithm based on particle filter and nearest neighbor data fusion for wireless sensor networks," *Remote Sensing*, vol. 22, no. 14, p. 5791, 2022.

[20] S. A. Loytty, N. Sirola, and R. Piche, "Consistency of three Kalman filter extensions in hybrid navigation," in *Proc. MDOI ENC*, 2005.

[21] C. D. Wann, Y. J. Yeh, and C. S. Hsueh, "Hybrid TDOA/AOA indoor positioning and tracking using extended Kalman filters," in *Proc. IEEE VTC*, 2006.

[22] B. S. Chen, C. Y. Yang, F. K. Liao, and J. F. Liao, "Mobile location estimator in a rough wireless environment using extended Kalman-based imm and data fusion," *IEEE Trans. Veh. Technol.*, vol. 58, no. 3, pp 1157–1169, Mar. 2009.

[23] C. T. Chiang, P. H. Tseng, and K. T. Feng, "Hybrid unified Kalman tracking algorithms for heterogeneous wireless location systems," *IEEE Trans. Veh. Technol.*, vol. 61, no. 2, pp. 702–715, Feb. 2012.

[24] G. D. Angelis, G. Baruffa, and S. Cacopardi, "GNSS/cellular hybrid positioning system for mobile users in urban scenarios," *IEEE Trans. Intell. Transp. Syst.*, vol. 14, no. 1, pp. 313–321, Mar. 2013.

[25] S. Wu, D. Xu, J. Tan, K. Xu, and H. Wang, "Two base station location techniques with adjusted measurements in circular scattering environments," *Int. J. Commun. Syst.*, vol. 29, no. 6, pp. 1073–1083, Apr. 2016.

[26] X. Sun, X. Gao, G. Y. Li, and W. Han, "Single-site localization based on a new type of fingerprint for massive mimo-ofdm systems," *IEEE Trans. Veh. Technol.*, vol. 67, no. 7, pp. 6134–6145, Jul. 2018.

[27] M. Ruble and I. Guvenc, "Wireless localization for mmwave networks in urban environments," *EURASIP J. Adv. Signal Process.*, vol. 35, pp. 61–35, Jun. 2018.

[28] A. Bourdoux, A. N. Barreto, and B. V. Liempd, "6G white paper on localization and sensing," in *arXiv: 2006.01779*, 2020.

[29] A. K. Abdulrhman, Y. E. M. Ali, and S. Younis, "Emerging development of wireless localization technologies aided with reconfigurable intelligent surfaces: A comprehensive survey," *NTU J. Eng. Technol.*, vol. 3, no. 2, pp. 55–74, 2024.

[30] S. Wu, D. Xu, S. Zhang, and D. Huang, "Single base station hybrid localization with scatter and angle of departure in circular scattering environment," *Annals Telecommun.*, vol. 71, pp. 649–655, Jul. 2016.

[31] S. Wu, S. Zhang, K. Xu, and D. Huang, "A weighting localization algorithm with LOS and one-bound NLOS identification in multipath environments," *J. Inf. Sci. Eng.*, vol. 35, no. 6, pp. 1209–1222, Nov. 2019.

[32] S. Wu, Q. Feng, W. Huang, and K. Xu, "Linear cooperative localization algorithm with TOA/AOA/AOD and multipath," in *Proc. WCCCT*, 2021.

[33] S. Wu, M. Li, M. Zhang, K. Xu, and J. Cao, "Single base station hybrid TOA/AOD/AOA localization algorithms with the synchronization error in dense multipath environment," *EURASIP J. Wireless Commun. Netw.*, vol. 4, pp. 1–21, Jan. 2022.

[34] B. Qamar, S. Saleh, M. Elhabiby, and A. Noureldin, "A step cLOSer towards 5G mmwave-based multipath positioning in dense urban environments," in *Proc. ION GNSS*, 2023.

[35] Z. Li, F. Jiang, H. Wymeersch, and F. Wen, "An iterative 5G positioning and synchronization algorithm in NLOS environments with multi-bounce paths," *IEEE Wireless Commun. Lett.*, vol. 12, no. 5, p. 804–808, May. 2023.

[36] B. Y. Shikur, M. Farmani, and T. Weber, "TOA/AOA/AOD-based 3-D mobile terminal tracking in NLOS multipath environments," in *Proc. WPNC*, 2012.

[37] Y. Zhicheng, J. Vinogradova, G. Fodor, and P. Hammarberg, "Vehicular positioning and tracking in multipath non-line-of-sight channels," in *Proc. IEEE VTC*, 2022.

[38] X. Zhao, F. Tian, and Z. Shao, "Localization and tracking using ODE-LSTM algorithm with non-line-of-sight channels," in *Proc. IEEE ISPA/BDCloud/SocialCom/SustainCom*, 2023.

[39] J. G. Andrews *et al.*, "Modeling and analyzing millimeter wave cellular systems," *IEEE Trans. Commun.*, vol. 65, no. 1, pp. 403–430, 2016.

[40] V. Y. Zhang and K. S. Wong, "Combined AOA and TOA NLOS localization with nonlinear programming in severe multipath environments," in *Proc. IEEE WCNC*, 2009.

[41] H. Miao, K. Yu, and M. J. Juntti, "Positioning for NLOS propagation: Algorithm derivations and Cramer–Rao bounds," *IEEE Trans. Veh. Technol.*, vol. 56, no. 5, pp. 2568–2580, Sep. 2007.

[42] C. K. Seow and S. Y. Tan, "Non-line-of-sight localization in multipath environments," *IEEE Trans. Mobile Computing*, vol. 7, no. 5, pp. 647–660, May. 2008.

[43] E. A. Wan and R. B. D. Merwe, "The unscented Kalman filter for nonlinear estimation," in *Proc. IEEE AS-SPCC*, 2000.
[44] M. Briers, S. R. Maskell, and R. Wright, "A Rao-Blackwellised unscented Kalman filter," in *Proc. IEEE FUSION*, 2003.
[45] S. A. Jazzar, J. Caffery, and H. R. You, "Scattering-model-based methods for TOA location in NLOS environments," *IEEE Trans. Vehicular Technology*, vol. 56, no. 2, pp. 583–593, Mar. 2007.
[46] S. Wu, D. Xu, and H. Wang, "Joint TOA/AOA location algorithms with two BSs in circular scattering environments," *WSEAS Trans. Commun.*, vol. 14, pp. 235–240, Jul. 2015.

Shixun Wu was born in HuBei, China. He received the B.S. and M.S. degrees in Applied Mathematics in 2006 and 2009, respectively. He received the PH.D. Degree in 2012 at the Department of Electrical and Computer Engineering, Central China Normal University, China. Currently he is a Vice-Professor at College of Information Science and Engineering, Chongqing Jiaotong University. He is also a Vice-Dean at Department of Communication Engineering. His current research interests include wireless localization, neural network localization, and wireless communication.

Miao Zhang (S'18, M'20) received his B.Sc. degree in Optical Information Science and Technology from Guizhou University, Guiyang, China, M.Sc. in Communications and Signal Processing from the University of Newcastle upon Tyne, Newcastle upon Tyne, UK, and the PhD from the University of York, York, UK in 2011, 2015 and 2020, respectively. He is currently an Associate Professor at the School of Information Science and Engineering, Chongqing Jiaotong University, Chongqing, China. His research interests are convex optimization techniques, intelligent reflecting surface assisted wireless networks, physical layer security and machine learning techniques for wireless communications.

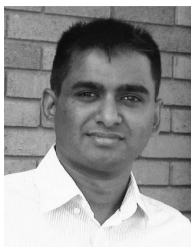

Kanapathippillai Cumanan (Senior Member, IEEE) received the B.Sc. degree (with first class Hons.) in Electrical and Electronic Engineering from the University of Peradeniya, Sri Lanka, in 2006 and the Ph.D. degree in Signal Processing for Wireless Communications from Loughborough University, Loughborough, U.K., in 2009. He is currently a Senior Lecturer with the School of Physics, Engineering and Technology, University of York, York, U.K. From March 2012 to November 2014, he was a Research Associate with the School of Electrical and Electronic Engineering, Newcastle University, Newcastle upon Tyne, U.K. Prior to this, he was with the School of Electronic, Electrical and System Engineering, Loughborough University, Loughborough, U.K. In 2011, he was an Academic Visitor with the Department of Electrical and Computer Engineering, National University of Singapore, Singapore. From January 2006 to August 2006, he was a Teaching Assistant with the Department of Electrical and Electronic Engineering, University of Peradeniya, Sri Lanka. He has authored or coauthored more than 100 journal articles and conference papers. His research interests include non-orthogonal multiple access (NOMA), cell-free massive MIMO, Open-RAN, WiFi networks, physical layer security, convex optimization techniques, and resource allocation techniques. He is currently an Associate Editor for IEEE JSAC-MACHINE LEARNING IN COMMUNICATIONS AND NETWORKS, IEEE WIRELESS COMMUNICATIONS LETTERS and IEEE OPEN JOURNAL OF COMMUNICATIONS SOCIETY. Dr. Cumanan was the recipient of an Overseas Research Student Award Scheme (ORSAS) from Cardiff University, Wales, U.K., where he was a Research Student between September 2006 to July 2007.

Kai Xu was born in 1970. He received M.S. degree in Control Theory and Control Engineering from Chongqing University in 2006. From 1993 to 2003, he was Senior Engineer in Xichang Satellite Launching Center. Since 2008, he is a Professor at college of Information Science and Engineering, Chongqing Jiaotong University. Prof. Xu is an Expert Commissioner of Chongqing Science and Technology Commission and Chongqing Construction Commission. His current research interests include fuzzy control, adaptive control, and intelligent algorithm.

Zhangli Lan was born in 1973. He received the B.S degree in communication from the Electronic Engineering College, Hefei, China, in 1997, the M.S. degree in Computer System Structure from Chongqing University, Chongqing, China, in 2004, and the Ph. D.degree in Computer Software and Theory from Chongqing University, Chongqing, China, 2008. From 2011, he has been a Professor with the School of Information Science and Engineering, Chongqing Jiaotong University, Chongqing, China. His current research interests include digital image processing, pattern recognition, and traffic information processing.